

Search for invisible decays of sub-GeV dark photons in missing-energy events at the CERN SPS

D. Banerjee,¹¹ V. Burtsev,⁹ D. Cooke,¹¹ P. Crivelli,¹¹ E. Depero,¹¹ A. V. Dermenev,⁴ S. V. Donskov,⁸ F. Dubinin,⁵ R. R. Dusaev,⁹ S. Emmenegger,¹¹ A. Fabich,³ V. N. Frolov,² A. Gardikiotis,⁷ S. N. Gninenko*,⁴ M. Hösgen,¹ V. A. Kachanov,⁸ A. E. Karneyeu,⁴ B. Ketzer,¹ D. V. Kirpichnikov,⁴ M. M. Kirsanov,⁴ I. V. Konorov,⁵ S. G. Kovalenko,¹⁰ V. A. Kramarenko,⁶ L. V. Kravchuk,⁴ N. V. Krasnikov,⁴ S. V. Kuleshov,¹⁰ V. E. Lyubovitskij,⁹ V. Lysan,² V. A. Matveev,² Yu. V. Mikhailov,⁸ V. V. Myalkovskiy,² V. D. Peshekhonov[†],² D. V. Peshekhonov,² O. Petuhov,⁴ V. A. Polyakov,⁸ B. Radics,¹¹ A. Rubbia,¹¹ V. D. Samoilenko,⁸ V. O. Tikhomirov,⁵ D. A. Tlisov,⁴ A. N. Toropin,⁴ A. Yu. Trifonov,⁹ B. Vasilishin,⁹ G. Vasquez Arenas,¹⁰ P. Ulloa,¹⁰ K. Zhukov,⁵ and K. Zioutas⁷
(The NA64 Collaboration[‡])

¹Universität Bonn, Helmholtz-Institut für Strahlen-und Kernphysik, 53115 Bonn, Germany

²Joint Institute for Nuclear Research, 141980 Dubna, Russia

³CERN, European Organization for Nuclear Research, CH-1211 Geneva, Switzerland

⁴Institute for Nuclear Research, 117312 Moscow, Russia

⁵P.N. Lebedev Physics Institute, Moscow, Russia, 119 991 Moscow, Russia

⁶Skobeltsyn Institute of Nuclear Physics, Lomonosov Moscow State University, Moscow, Russia

⁷Physics Department, University of Patras, Patras, Greece

⁸State Scientific Center of the Russian Federation Institute for High Energy Physics of National Research Center 'Kurchatov Institute' (IHEP), 142281 Protvino, Russia

⁹Tomsk Polytechnic University, 634050 Tomsk, Russia

¹⁰Universidad Técnica Federico Santa María, 2390123 Valparaíso, Chile

¹¹ETH Zürich, Institute for Particle Physics, CH-8093 Zürich, Switzerland

(Dated: October 14, 2016)

We report on a direct search for sub-GeV dark photons (A') which might be produced in the reaction $e^- Z \rightarrow e^- Z A'$ via kinetic mixing with photons by 100 GeV electrons incident on an active target in the NA64 experiment at the CERN SPS. The A' s would decay invisibly into dark matter particles resulting in events with large missing energy. No evidence for such decays was found with $2.75 \cdot 10^9$ electrons on target. We set new limits on the $\gamma - A'$ mixing strength and exclude the invisible A' with a mass $\lesssim 100$ MeV as an explanation of the muon $g_\mu - 2$ anomaly.

PACS numbers: 14.80.-j, 12.60.-i, 13.20.Cz, 13.35.Hb

Despite the intensive searches at the LHC and in non-accelerator experiments Dark Matter (DM) still is a great puzzle. Though stringent constraints obtained on DM coupling to Standard Model (SM) particles ruled out many DM models, little is known about the origin and dynamics of the dark sector itself. One difficulty so far is that DM can be probed only through its gravitational interaction. An exciting possibility is that in addition to gravity, a new force between the dark sector and visible matter transmitted by a new vector boson A' (dark photon) might exist. Such A' could have a mass $m_{A'} \lesssim 1$ GeV - associated with a spontaneously broken gauged $U(1)_D$ symmetry- and couple to the SM through kinetic mixing with the ordinary photon, $-\frac{1}{2}\epsilon F_{\mu\nu} A'^{\mu\nu}$, parameterized by the mixing strength $\epsilon \ll 1$ [1–3]. This has motivated a worldwide theoretical and experimental effort towards dark forces and other portals between the visible and dark sectors, see [4, 5] for a review. An additional motivation has been provided by hints on astrophysical

signals of dark matter [6], as well as the 3.6σ deviation from the SM prediction of the muon anomalous magnetic moment $g_\mu - 2$ [7], which can be explained by a sub-GeV A' with the coupling $\epsilon \simeq 10^{-3}$ [8–10]. Such small values of ϵ could naturally be obtained from loop effects of particles charged under both the dark and SM $U(1)$ interactions with a typical 1-loop value $\epsilon = eg_D/16\pi^2$ [3], where g_D is the coupling constant of the $U(1)_D$ gauge interactions. Various theoretical and phenomenological aspects of light vector bosons very weakly coupled to quarks and leptons have been also studied in pioneer papers by Fayet [11].

If the A' is the lightest state in the dark sector, then it would decay mainly visibly, i.e., typically to SM leptons $l = e, \mu$ or hadrons, which could be used to detect it. Previous beam dump [12]–[27], fixed target [28–30], collider [31–33], and rare meson decay [34]–[43] experiments have already put stringent constraints on the mass $m_{A'}$ and ϵ of such dark photons excluding, in particular, the parameter region favored by the $g_\mu - 2$ anomaly.

However, in the presence of light dark states, in particular dark matter, with the masses $< m_{A'}$, the A' would predominantly decay invisibly into those particles provided that $g_D > \epsilon e$. Models introducing such invisible

*Corresponding author, Sergei.Gninenko@cern.ch

[†]Deceased

[‡]<https://na64.web.cern.ch>

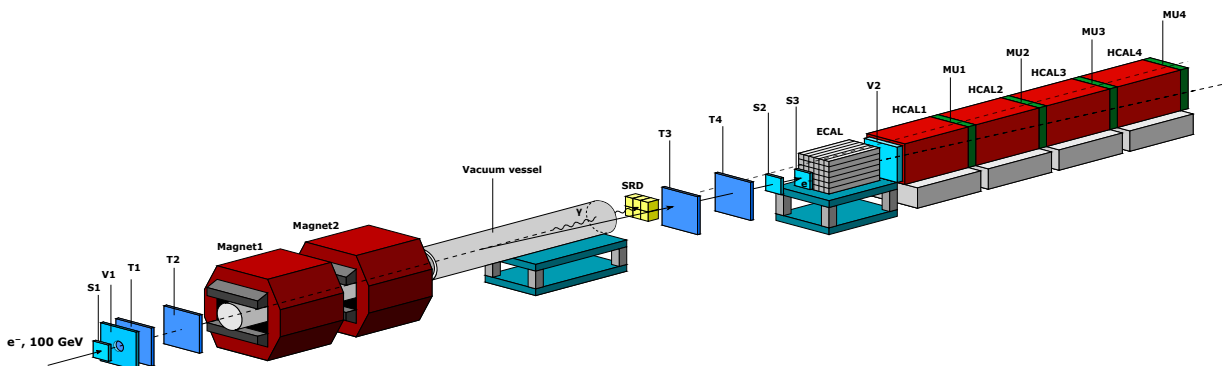


FIG. 1: Schematic illustration of the setup to search for $A' \rightarrow \text{invisible}$ decays of the bremsstrahlung A' s produced in the reaction $eZ \rightarrow eZA'$ of 100 GeV e^- incident on the active ECAL target.

A' offer new intriguing possibilities to explain the $g_\mu - 2$ and various other anomalies [44] and are subject to different experimental constraints [45–48]. The most severe limits on the invisible sub-GeV A' s decays have been obtained from the results of beam dump experiments LSND [49] and E137 [50], under assumptions on the strength of the coupling g_D , and properties of the DM decay particles. In this Letter we report the first results from the experiment NA64 specifically designed for a direct search of the $A' \rightarrow \text{invisible}$ decay at the CERN SPS.

The method of the search is as follows [51, 52]. If the A' exists it could be produced via the kinetic mixing with bremsstrahlung photons in the reaction of high-energy electrons scattering off nuclei of an active target of a hermetic detector, followed by the prompt $A' \rightarrow \text{invisible}$ decay into dark matter particles (χ):

$$e^- Z \rightarrow e^- ZA'; A' \rightarrow \text{invisible} \quad (1)$$

A fraction f of the primary beam energy $E_{A'} = fE_0$ is carried away by χ 's which penetrate the detector without interactions resulting in an event with zero-energy deposition. While the remaining part $E_e = (1 - f)E_0$ is deposited in the target by the scattered electron. Thus, the occurrence of A' produced in the reaction (1) would appear as an excess of events whose signature is a single e-m shower in the target with energy E_e accompanied by a significant missing energy $E_{\text{miss}} = E_{A'} = E_0 - E_e$ above those expected from backgrounds. Here we assume that the χ s have to traverse the detector without decaying visibly in order to give a missing energy signature. No any other assumptions on the nature of the $A' \rightarrow \text{invisible}$ decay are made.

The NA64 detector is schematically shown in Fig. 1. The experiment employed the upgraded 100 GeV electron beam from the H4 beamline. The beam has a maximal intensity $\simeq (3 - 4) \cdot 10^6$ per SPS spill of 4.8 s produced by the primary 450 GeV/c proton beam with an intensity of few 10^{12} protons on target. The detector utilized the beam defining scintillator (Sc) counters S1-S3, and magnetic spectrometer consisting of two successive dipole magnets with the integral magnetic field of $\simeq 7$ T-m and

a low-material-budget tracker. The tracker was a set of two upstream Micromegas chambers (T1, T2) and two downstream GEM stations (T3, T4) allowing the measurements of e^- momenta with the precision $\delta p/p \simeq 1\%$ [53]. The magnets also served as an effective filter rejecting low energy component of the beam. To enhance the electron identification the synchrotron radiation (SR) emitted by electrons was used for their efficient tagging. A 15 m long vacuum vessel between the magnets and the ECAL was installed to minimize absorption of the SR photons detected immediately at the downstream end of the vessel with a SR detector (SRD), which was either an array of BGO crystals or a PbSc sandwich calorimeter of a very fine segmentation [51]. By using the SRD the initial level of the hadron contamination in the beam $\pi/e^- \lesssim 10^{-2}$ was further suppressed by a factor $\simeq 10^3$. The detector was also equipped with an active target, which is an electromagnetic (e-m) calorimeter (ECAL) for measurement of the electron energy with the accuracy $\delta E/E \simeq 10\%/\sqrt{E}$. The ECAL is a matrix of 6×6 Shashlik-type modules assembled from Pb and Sc plates with wave-shifting fiber read-out. Each module is $\simeq 40$ radiation lengths. Downstream the ECAL the detector is equipped with a high-efficiency veto counter V2, and a massive, hermetic hadronic calorimeter (HCAL) of $\simeq 30$ nuclear interaction lengths. The HCAL served as a dump to completely absorb and measure the energy of hadronic secondaries produced in the $e^- A \rightarrow \text{anything}$ interactions in the target. Four muon plane counters, MU1-MU4, located between the HCAL modules were used for the muon identification in the final state. The events were collected with the hardware trigger requiring an intime cluster in the ECAL with the energy $E_{\text{ECAL}} \lesssim 80$ GeV. The results reported here came mostly from a set of data in which $n_{\text{eot}} = 1.88 \cdot 10^9$ of electrons on target (eot) were collected with the beam intensity $\simeq 1.4 \cdot 10^6$ e^- per spill with the PbSc calorimeter. While a smaller sample of $n_{\text{eot}} = 0.87 \cdot 10^9$ and an intensity $I_e = 0.3 \cdot 10^6$ e^- was also recorded with the BGO detector. Data of these two runs (hereafter called the BGO and PbSc run) were analyzed with similar selection criteria and finally summed up, taking into account the corresponding normalization

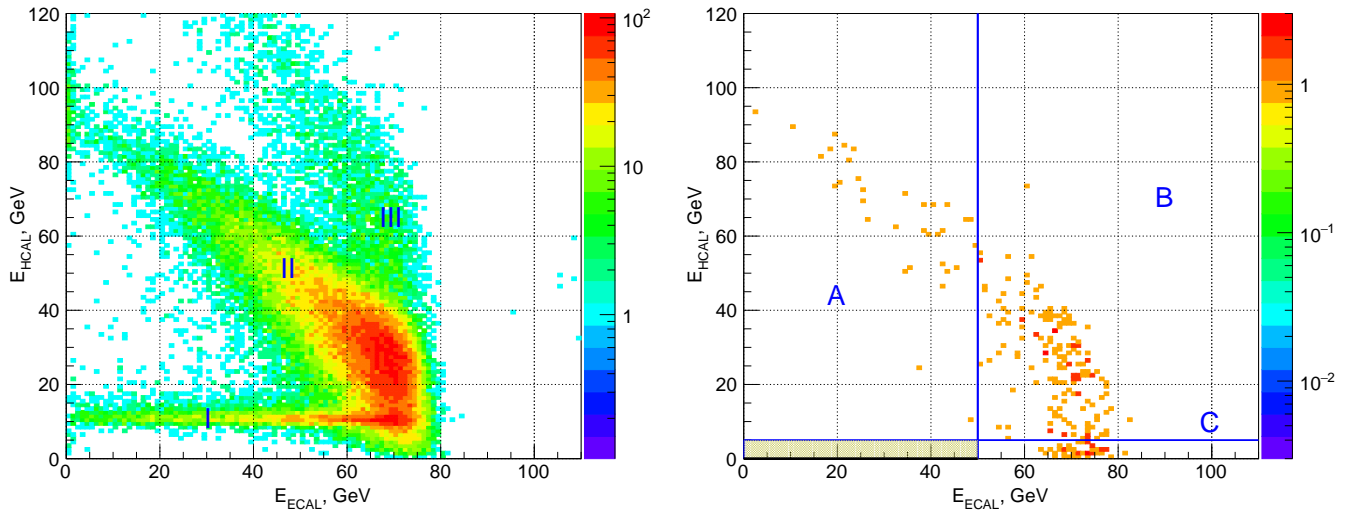


FIG. 2: The left panel shows the measured distribution of events in the $(E_{ECAL}; E_{HCAL})$ plane from the combined BGO and PbSc run data at the earlier phase of the analysis. Another plot shows the same distribution after applying all selection criteria. The dashed area is the signal box region which is open. The side bands A and C are the one used for the background estimate inside the signal box. For illustration purposes the size of the signal box along E_{HCAL} -axis is increased by a factor five.

factors.

In order to avoid biases in the determination of selection criteria for candidate events, a blind analysis was performed. Candidate events are expected to have the missing energy in the range $50 < E_{miss} < 100$ GeV, which was defined by taking into account the energy spectrum of A' 's emitted in the primary reaction (1) by e^\pm from the e-m shower generated by the beam e^- 's in the ECAL target [54]. Events from a signal box ($E_{ECAL} < 50$ GeV; $E_{HCAL} < 1$ GeV) were excluded from the analysis of the data until the validity of the background estimate in this region was established. For the selection criteria optimization, 10% of the data was used, while the full sample was used for the background estimate. The number of signal candidate events were counted after unblinding. A detailed Geant4 based Monte Carlo (MC) simulation was used to study the detector performance and acceptance, to simulate background sources, and to select cuts and estimate the reconstruction efficiency.

The left panel in Fig. 2 shows the distribution of the events from the reaction $e^- Z \rightarrow anything$ in the $(E_{ECAL}; E_{HCAL})$ plane measured with $2.75 \cdot 10^9$ eot. Here, E_{HCAL} is the sum of the energy deposited in the first two HCAL modules. About $5 \cdot 10^4$ events were selected with the loose cut requiring in-time energy deposition in the SRD within the SR range emitted by e^- . Events from the area I in Fig. 2 originate from the rare QED dimuon production, dominated by the reaction $e^- Z \rightarrow e^- Z \gamma; \gamma \rightarrow \mu^+ \mu^-$, of the muon pair photo-production by a hard bremsstrahlung photon conversion on a target nuclei and characterized by the energy of $\simeq 10$ GeV deposited by the dimuon pair in the HCAL.

This process was used as a benchmark allowing to verify the reliability of the MC simulation and estimate the systematic uncertainties in the signal reconstruction efficiency in the energy range predicted by simulations. The same selection cuts were applied to both signal and reference channel, in order to cross-check systematic uncertainties. The dimuon production was also used as a reference for the background prediction. The region II shows the SM events from the hadron electroproduction in the target which satisfy the energy conservation $E_{ECAL} + E_{HCAL} \simeq 100$ GeV within the energy resolution of the detectors. The leak of these events to the signal box due to the energy resolution is was found to be negligible. The events from the region III whose fraction is a few 10^{-2} are mostly due to pile-up of e^- and beam hadrons.

The candidate events were selected with the criteria chosen to maximize the acceptance for MC signal events and to minimize the numbers of background events, respectively. The following selection criteria were applied: i) The incoming particle track should have a small angle w.r.t. the beam axis to reject large angle tracks from the upstream e^- interactions. ii) The energy deposited in the SRD detector should be within the SR range emitted by e^- 's and in-time with the trigger; iii) The lateral and longitudinal shape of the shower in the ECAL should be consistent with the one expected for the signal shower [54]; iv) No activity in V2. Only $\simeq 300$ events passed these criteria from combined BGO and PbSc runs.

The search for the $A' \rightarrow invisible$ decays requires particular attention to backgrounds. Every process with a track and a single e-m cluster in the

TABLE I: Expected numbers of events in the signal box from different background sources estimated for $2.75 \cdot 10^9$ eot.

Source of background	Events
loss of e^- energy due to punchthrough γ s	< 0.001
loss of hadrons from $e^-Z \rightarrow e^- + \text{hadrons}$	< 0.01
loss or $\mu \rightarrow e\nu\nu$ decays	
of muons from $e^-Z \rightarrow e^-Z\gamma; \gamma \rightarrow \mu^+\mu^-$	< 0.01
e^- interactions in the beamline materials	0.03
$\mu \rightarrow e\nu\nu, \pi, K \rightarrow e\nu, K_{e3}$ decays	0.03
pile-up of low energy e^- and μ, π, K followed by their decays	0.05
μ, π, K interactions in the target	0.02
Total	0.15

ECAL was considered as a potential source of background. There are several sources which may fake the $A' \rightarrow \text{invisible}$ signal, e.g. upstream e^- interactions, $\mu \rightarrow e\nu\nu, \pi, K \rightarrow e\nu, K_{e3}$ decays in-flight, energy leakage from particle punch-through in the HCAL, processes due to pile-up of two or more particles, and instrumental effects due to energy loss through cracks in the upstream detector coverage. The selection cuts to eliminate these backgrounds have been chosen such that they do not affect the shape of the true E_{miss} spectrum.

Two independent methods were used for the background estimation in the signal region. The first method is based on the MC. Due to the small coupling strength of the A' reaction (1) occurs typically with a rate $\lesssim 10^{-9}$ per incoming electron. To study the SM distribution and background at this level is very time-consuming. Consequently, we have evaluated with MC all known backgrounds to the extent that it is possible. Events from particle interactions or decays in the beam line, pile-up activity created from them, hadron punch-through from the target and the HCAL were included in the simulation of all background events. Small event-number backgrounds such as the decays of the beam μ, π, K or μ from the reaction of dimuon production were simulated with the full statistics of the data. Large event-number processes, e.g. upstream beam interactions, punch-through of secondary hadrons were also studied extensively, although simulated samples with statistics similar to the data were not feasible. To eliminate possible instrumental effects not present in the MC, the uniformity scan of the central part of the ECAL target was performed with e^- by using T3 and T4. We also examined the number of events observed in several regions around the signal box, which were statistically consistent with the estimates.

Two largest sources of background are expected from the beam μ, π, K decays in-flight. In one case, when, e.g. a pion passes through the vacuum vessel it could knock electrons off the downstream window, which hit the SRD creating a fake tag for a 100 GeV e^- . Then the pion could decay into $e\nu$ in the upstream ECAL region thus producing the fake signal. Similar background is caused

by the pile-up of an electron from the low-energy beam tail ($\lesssim 60-80$ GeV) and a beam $\mu, \pi, \text{ or } K$. The electron could emit the amount of SR energy above the threshold which is detected in the SRD as a tag of 100 GeV e^- and then is deflected by the magnets out of the detector's acceptance angle. While the accompanied muon or hadron could then decay in flight. For both sources the dominant background came from the K_{e3} decays. The mistakenly tagged $\mu, \text{ and } \pi \text{ and } K$ could also interact in the target producing an e-m like cluster below 50 GeV though the $\mu Z \rightarrow \mu Z\gamma$ or π, K charge-exchange reactions in the target, accompanied by the poorly detected scattered $\mu, \text{ or secondary hadrons, respectively. Another background is due to } e^- \text{ interactions with the beamline materials resulting in } e^- \text{ energy loss. Table I summarizes the conservatively estimated number of background events inside the signal box. The expected number of background events is } 0.15 \pm 0.03(\text{stat}) \pm 0.06(\text{syst}). \text{ The systematic error includes the uncertainties in the amount of passive material for upstream } e^- \text{ interactions, and in the cross sections of the of } \pi, K \text{ charge-exchange reactions on lead (30\%).}$

The second method used the background estimate extracted from the data themselves. MC signal events and the background extrapolated from sidebands A and C shown in the right panel of Fig. 2 were used. Events in the region A are pure neutral hadronic secondaries produced by electrons in the ECAL target, while events from the region C are likely from the e^- interactions in the downstream part of the beamline accompanied by bremsstrahlung photons absorbed in the HCAL. The yield of the background events was estimated by extrapolating the observed events to the signal region assessing the systematic uncertainties by varying the background fit models. Using this we obtained a second background estimate of 0.4 ± 0.3 events. The background estimates with the two methods are in agreement with each other within errors. After determining all the selection criteria and estimating background levels, we examined the events in the signal box and found no candidates, as shown in Fig. 2. The conclusion that the background is small is confirmed by the data.

The $m_{A'}$ -dependent upper limit on the mixing ϵ is calculated as follows. For a given number n_{eot} and the mass $m_{A'}$, the number of signal events $N_{A'}$ expected from the reaction (1) in the signal box is given by:

$$N_{A'} = n_{eot} \cdot n_{A'}(\epsilon, m_{A'}, \Delta E_{A'}) \cdot \epsilon_{A'}(m_{A'}, \Delta E_{A'}) \quad (2)$$

where $n_{A'}(\epsilon, m_{A'}, \Delta E_{A'})$ is the yield of A' s with the coupling ϵ , mass $m_{A'}$, and energy in the range $\Delta E_{A'}, 0.5E_0 < E_{A'} < E_0$, per e-m shower generated by a single 100 GeV electron in the ECAL [54]. These events corresponds to the missing energy $0.5E_0 < E_{miss} < E_0$. The overall signal efficiency, $\epsilon_{A'}$ is weakly $m_{A'}, E_{A'}$ dependent and is given by the product of efficiencies accounting for the NA64 geometrical acceptance (0.97), the analysis efficiency ($\simeq 0.8$) which is slightly $m_{A'}$ dependent, veto V2 (0.96) and HCAL signal efficiency (0.94) and the accep-

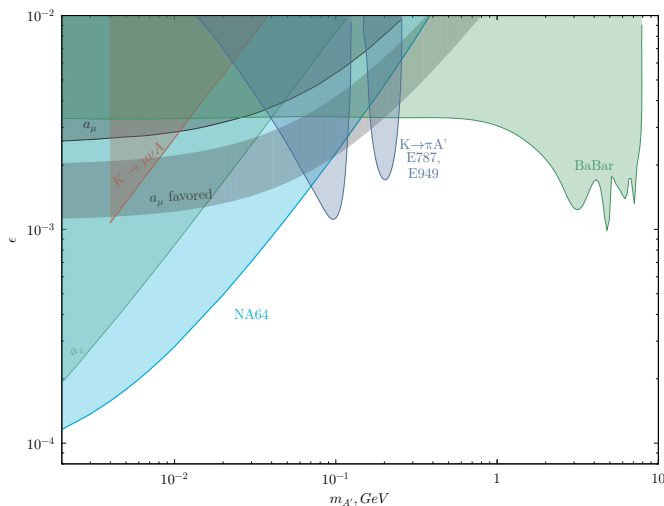


FIG. 3: The NA64 90 % C.L. exclusion region in the $(m_{A'}, \epsilon)$ plane. Constraints from the BaBar [48, 55], and E787+ E949 experiments [47, 56], as well as muon α_μ favored area are also shown. Here, $\alpha_\mu = \frac{g_\mu - 2}{2}$. For more limits obtained from indirect searches and planned measurements see e.g. Refs. [5].

tance loss due to pile-up ($\simeq 8\%$ for BGO and $\simeq 7\%$ for PbSc runs). The number of collected $n_{eot} = 2.75 \cdot 10^9$ was estimated based on the recorded number of reference events from the e-m e^-Z interactions in the target taking into account dead time. The acceptance of the signal events was evaluated by taking all relevant momentum and angular distributions into account. The A' yield calculated as described in Ref.[54] was cross-checked with calculations of Ref.[55]. The $\simeq 10\%$ discrepancy between these two calculations was accounted for as systematic uncertainty in $n_{A'}(\epsilon, m_{A'}, \Delta E_{A'})$ due to a possible difference in treatment of the e-m shower development. To estimate additional uncertainty in the A' yield prediction, the cross-check between a clean sample of $\simeq 5 \cdot 10^3$ observed and MC predicted $\mu^+\mu^-$ events with $E_{ECAL} \lesssim 60$ GeV was made, resulting in $\simeq 15\%$ difference in the dimuon yield. The number of A' and dimuon events are both proportional to the square of the Pb nuclear form factor $F(q^2)$ and are sensitive to its shape. As the mass ($m_{A'} \simeq m_\mu$) and q^2 ($q \simeq m_{A'}/E_{A'} \simeq m_\mu^2/E_\mu$) ranges for both reactions are similar, the observed difference can be interpreted as due to the accuracy of the dimuon yield calculation for heavy nuclei and, thus can be conservatively accounted for as additional systematic uncertainty in $n_{A'}(\epsilon, m_{A'}, \Delta E_{A'})$. The V2 and HCAL signal efficiency was defined as a fraction of events below

the corresponding zero-energy thresholds. The shape of the energy distributions in these detectors from the leak of signal shower energy from the ECAL was simulated for different A' masses [54] and cross-checked with measurements at the e^- beam. The uncertainty in the V2 and HCAL efficiency for the signal events, dominated mostly by the pile-up effect from penetrating hadrons in the high intensity PbSc run, was estimated to be $\simeq 3\%$. The trigger (SRD) efficiency is measured in unbiased random samples of events that bypass the trigger (SRD) selection and the uncertainty is 2% (3%). Other effects, e.g. e^- loss due to conversion into $e^-\gamma$ pair in the upstream detector material were measured to be $\lesssim 3\%$ (2% uncertainty). Finally, the dominant source of systematic errors on the expected number of signal events comes from the uncertainty in the estimate of the yield $n_{A'}(\epsilon, m_{A'}, \Delta E_{A'})$ (19%). The overall signal efficiency $\epsilon_{A'}$ varied from 0.69 ± 0.09 to 0.55 ± 0.07 decreasing for the higher A' masses.

In accordance with the CL_s method [57], for zero observed events the 90% C.L. upper limit for the number of signal events is $N_{A'}^{90\%}(m_{A'}) = 2.3$. Taking this and Eq.(2) into account and using the relation $N_{A'}(m_{A'}) < N_{A'}^{90\%}(m_{A'})$ results in the 90% C.L. exclusion area in the $(m_{A'}, \epsilon)$ plane shown in Fig. 3. The limits are determined mostly by the number of accumulated eot. These results exclude the invisible A' as an explanation of the $g_\mu - 2$ muon anomaly for the masses $m_{A'} \lesssim 100$ MeV. Moreover, the results also allow to restrict other models with light particles interacting with electron and decaying predominantly to invisible modes. For instance for light scalar particle s with the interaction $L_{es} = s\bar{e}(h_s + h_{as}i\gamma_5)e$ the bound on ϵ_s ($\epsilon_s^2 \alpha \equiv \frac{h_s^2 + h_{as}^2}{4\pi}$) is approximately 1.5 times weaker than the one obtained on ϵ for the model with light vector bosons [58]. Here h_s and h_{as} are scalar and pseudoscalar Yukawa coupling constants of the light scalar field s with electron field e , respectively.

We gratefully acknowledge the support of the CERN management and staff and the technical staffs of the participating institutions for their vital contributions. This work was supported by the HISKP, University of Bonn (Germany), JINR (Dubna), MON and RAS (Russia), SNF (Switzerland), and grants FONDECYT 1140471 and 1150792, Ring ACT1406 and Basal FB0821 CONICYT (Chile). Part of the work on MC simulations was supported by the RSF grant 14-12-01430. We thank S. Andreas and A. Ringwald for their contribution at the earlier stage of the project, and V.Yu. Karjavin, J. Novy, V.I. Savrin, and I.I. Tkachev for their help. We thank COMPASS DAQ group and the Institute for Hadronic Structure and Fundamental Symmetries of TU Munich for the technical support.

[1] L. B. Okun, Sov. Phys. JETP **56** (1982) 502 [Zh. Eksp. Teor. Fiz. **83** (1982) 892].
 [2] P. Galison and A. Manohar, Phys. Lett. B **136**, 279

(1984).

[3] B. Holdom, Phys. Lett. B **166**, 196 (1986).
 [4] J. Jaeckel and A. Ringwald, Ann. Rev. Nucl. Part. Sci.

- 60**, 405 (2010).
- [5] J. Alexander et al., arXiv:1608.08632.
- [6] N. Arkani-Hamed, D. P. Finkbeiner, T. R. Slatyer, and N. Weiner, Phys. Rev. D **79**, 015014 (2009).
- [7] G. W. Bennett et al. (Muon G-2 Collaboration), Phys. Rev. D **73**, 072003 (2006).
- [8] S.N.Gninenko and N.V.Krasnikov, Phys. Lett. B **513**, 119 (2001).
- [9] P.Fayet, Phys. Rev. D **75**, 115017 (2007).
- [10] M. Pospelov, Phys. Rev. D **80**, 095002 (2009).
- [11] P. Fayet, Phys. Lett. B **95**, 285 (1980); Nucl. Phys. B **347**, 743 (1980); Phys. Rev. D **70** 023514 (2004); Phys. Rev. D **74** 054034 (2006).
- [12] J. D. Bjorken, R. Essig, P. Schuster, and N. Toro, Phys. Rev. D **80**, 075018 (2009).
- [13] F. Bergsma et al. (CHARM Collaboration), Phys. Lett. **166B**, 473 (1986).
- [14] A. Konaka et al., Phys. Rev. Lett. **57**, 659 (1986).
- [15] E. M. Riordan et al., Phys. Rev. Lett. **59**, 755 (1987).
- [16] J. D. Bjorken, S. Ecklund, W. R. Nelson, A. Abashian, C. Church, B. Lu, L. W. Mo, T. A. Nunamaker, and P. Rassmann, Phys. Rev. D **38**, 3375 (1988).
- [17] A. Bross, M. Crisler, S. H. Pordes, J. Volk, S. Errede, and J. Wrbanek, Phys. Rev. Lett. **67**, 2942 (1991).
- [18] M. Davier and H. Nguyen Ngoc, Phys. Lett. B **229**, 150 (1989).
- [19] C. Athanassopoulos et al. (LSND Collaboration), Phys. Rev. C **58**, 2489 (1998).
- [20] P. Astier et al. (NOMAD Collaboration), Phys. Lett. B **506**, 27 (2001).
- [21] S. Adler et al. (E787 Collaboration), Phys. Rev. D **70**, 037102 (2004).
- [22] A. V. Artamonov et al. (BNL-E949 Collaboration), Phys. Rev. D **79**, 092004 (2009).
- [23] R. Essig, R. Harnik, J. Kaplan, and N. Toro, Phys. Rev. D **82**, 113008 (2010).
- [24] J. Blumlein and J. Brunner, Phys. Lett. B **701**, 155 (2011).
- [25] S. Gninenko, Phys. Lett. B **713**, 244 (2012).
- [26] J. Blumlein and J. Brunner, Phys. Lett. B **731**, 320 (2014).
- [27] S. Andreas, C. Niebuhr, and A. Ringwald, Phys. Rev. D **86**, 095019 (2012).
- [28] S. Abrahamyan et al. (APEX Collaboration), Phys. Rev. Lett. **107**, 191804 (2011).
- [29] H. Merkel et al., Phys. Rev. Lett. **112**, 221802 (2014).
- [30] H. Merkel et al. (A1 Collaboration), Phys. Rev. Lett. **106**, 251802 (2011).
- [31] B. Aubert et al. (BABAR Collaboration), Phys. Rev. Lett. **103**, 081803 (2009).
- [32] D. Curtin et al., Phys. Rev. D **90**, 075004 (2014).
- [33] J. P. Lees et al. (BABAR Collaboration), Phys. Rev. Lett. **113**, 201801 (2014).
- [34] G. Bernardi, G. Carugno, J. Chauveau, F. Dicarolo, M. Dris et al., Phys. Lett. **166B**, 479 (1986).
- [35] R. Meijer Drees et al. (SINDRUM I Collaboration), Phys. Rev. Lett. **68**, 3845 (1992).
- [36] F. Archilli et al. (KLOE-2 Collaboration), Phys. Lett. B **706**, 251 (2012).
- [37] S. N. Gninenko, Phys. Rev. D **85**, 055027 (2012).
- [38] D. Babusci et al. (KLOE-2 Collaboration), Phys. Lett. B **720**, 111 (2013).
- [39] P. Adlarson et al. (WASA-at-COSY Collaboration), Phys. Lett. B **726**, 187 (2013).
- [40] G. Agakishiev et al. (HADES Collaboration), Phys. Lett. B **731**, 265 (2014).
- [41] A. Adare et al. (PHENIX Collaboration), Phys. Rev. C **91**, 031901 (2015).
- [42] J. R. Batley et al. (NA48/2 Collaboration), Phys. Lett. B **746**, 178 (2015).
- [43] A. Anastasi et al. (KLOE-2 Collaboration), Phys. Lett. B **757**, 356 (2016).
- [44] H. S. Lee, Phys. Rev. D **90**, 091702 (2014).
- [45] E. Izaguirre, G. Krnjaic, P. Schuster, and N. Toro, Phys. Rev. D **88**, 114015 (2013).
- [46] M. D. Diamond and P. Schuster, Phys. Rev. Lett. **111**, 221803 (2013).
- [47] H. Davoudiasl, H. S. Lee, and W. J. Marciano, Phys. Rev. D **89**, 095006 (2014).
- [48] B. Aubert *et al.* [BaBar Collaboration], arXiv:0808.0017 [hep-ex].
- [49] B. Batell, M. Pospelov, and A. Ritz, Phys. Rev. D **80**, 095024 (2009).
- [50] B. Batell, R. Essig, and Z. Surujon, Phys. Rev. Lett. **113**, 171802 (2014).
- [51] S. N. Gninenko, Phys. Rev. D **89**, 075008 (2014).
- [52] S. Andreas *et al.*, arXiv:1312.3309 [hep-ex].
- [53] D. Banerjee, P. Crivelli and A. Rubbia, Adv. High Energy Phys. **2015** 105730, (2015).
- [54] S.N. Gninenko, N.V. Krasnikov, M.M. Kirsanov, and D.V. Kirpichnikov, arXiv:1604.08432.
- [55] E. Izaguirre, G. Krnjaic, P. Schuster and N. Toro, Phys. Rev. D **91**, no. 9, 094026 (2015).
- [56] R. Essig, J. Mardon, M. Papucci, T. Volansky, and Y. M. Zhong, J. High Energy Phys. **11** 167, (2013).
- [57] A.L. Read, J. Phys. G **28** 2693, (2002).
- [58] NA64 collaboration. Paper in preparation.